CANCER GENOMICS & PROTEOMICS *20*: 281-297 (2023)
doi:10.21873/cgp.20381

Knockdown of G Protein-coupled Estrogen Receptor 1 (GPER1) Enhances Tumor-supportive Properties in Cervical Carcinoma Cells

SOPHIA RUCKRIEGL, JOHANNA LORIS, KATSIARYNA WERT, GERD BAUERSCHMITZ, JULIA GALLWAS and CARSTEN GRÜNDKER

Department of Gynecology and Obstetrics, University Medical Center Göttingen, Göttingen, Germany

Abstract. *Background/Aim: A wide variety of answers can be found regarding the question of whether G-protein-coupled estrogen receptor 1 (GPER1) is tumor supportive or tumor suppressive. In cervical carcinoma (CC), the function of GPER1 is poorly understood. In this work, we aimed to clarify what role GPER1 plays in CC, tumor promoting of tumor suppressive. Materials and Methods: Transient GPER1 silencing was conducted using RNAi and approved by RT-qPCR. Clonogenic potential was tested by colony and sphere formation. Expression of SERPINE1/PAI-1 was quantified by RT-qPCR and Western blot. Morphological changes were analyzed using Phalloidin staining. Localization of GPER1 in tumor spheres was examined by immunofluorescence. Results: After GPER1 knockdown, more colonies formed in HeLa and SiHa, and larger colonies formed in C33-A and SiHa CC cells. Size of HeLa and SiHa tumor spheres was also increased. In addition, number of HeLa tumor spheres was elevated, and larger secondary colonies were present. C33-A only formed tumor sphere-like clusters showing no differences in number and size. Phalloidin staining revealed greater cellular length-to-width ratio and increased average filopodia length. Expression of SERPINE1/PAI-1 was increased in HeLa and decreased in C33-A. In SiHa cells, SERPINE1 was slightly decreased, whereas the protein PAI-1 was increased. Strong expression of GPER1 was detectable in peripheral areas and in sprouts of tumor spheres. Conclusion: GPER1 appears to be tumor suppressive in CC, as GPER1 knockdown provoked increased stem cell properties and increased migration/invasion. EMT also appears to be enhanced. Of interest is the increase in SERPINE1/PAI-1 expression after GPER1 knockdown.*

Correspondence to: Prof. Dr. Carsten Gründker, Department of Gynecology and Obstetrics, Robert-Koch-Street 40, 37075 Göttingen, Germany. Tel: +49 (0)5513969810, e-mail: grundker@med.uni-goettingen.de

Key Words: G-protein-coupled estrogen receptor 1, GPER1, cervical carcinoma, tumor suppressor, SERPINE1/PAI-1.

With around 600,000 new cases and around 340,000 deaths per year, cervical cancer (CC) is the fourth most common cancer in women. It is the most common gynecological tumor (1). CC develops gradually from cervical intraepithelial neoplasia (CIN1-3) which in turn is caused by human papillomavirus (HPV) infection (2, 3). HPV-DNA can be detected in about 95% of invasive CCs and there is a strong association between persistent infection with high-risk HPV types and the development of CC (4). CCs are divided into squamous cell carcinomas and adenocarcinomas. Squamous cell carcinomas are represented in the majority with about 80%, while adenocarcinomas make up 5-20% of the carcinomas (5, 6). The origin of most CC is the transformation zone, which is located on the surface of the portio in younger women and more endocervically in postmenopausal women (7).

The G-protein-coupled estrogen receptor 1 (GPER1) is a seven-transmembrane-domain receptor responsible for many rapid estrogen-induced effects (8). GPER1 acts as a non-genomic signal transducer, which, among other things, has various influences on proliferation or cell cycle processes through an increase in cAMP production, calcium mobilization, activation of epidermal growth factor receptor (EGFR) and participation in the MAP kinase signaling pathway (9). GPER1 ligands include the physiologically occurring estrogens estrone and estradiol, but also drugs such as tamoxifen, raloxifene or bisphenol A. Another ligand that has an agonistic effect on GPER1 is the agonist G-1, which was first produced synthetically in 2006. G-1 is the first ligand that binds selectively to GPER1 and not to other estrogen receptors (10). The estrogen estriol (11) and the two synthetically produced antagonists G15 and G36 have an

antagonistic effect on GPER1 (9). Referring to uterine tissue, GPER1 was found in uterine adenocarcinoma (12). But also, in the squamous cell carcinoma of the cervix, GPER1 was detected in the majority of carcinomas, whereby GPER1 is present in the membrane of the cells as well as in the cytoplasm both in adeno- and in squamous cell carcinoma of the cervix. In most cases, the expression of GPER1 in the membrane and the cytoplasm was measured simultaneously (13). Especially in the HeLa, SiHa and C33-A CC cells that are used in this work, it was shown that GPER1 is expressed (14). Most of the knowledge on GPER1 so far is from studies on breast cancer (15). It has been found that GPER1 plays an important role in the progression, migration, and possible resistance to therapies of carcinoma cells (15). Overall patient survival has also been associated with GPER1 in ovarian, endometrial and breast cancer (9). It is interesting that GPER1 achieves tumor supportive but also tumor suppressive effects in a wide variety of cancer entities and even in the same tumor entity, with a particular focus on breast cancer in the gynecological field (15). For this reason, the focus of our work, namely the role of GPER1 in cervical carcinoma, is of great relevance. This is particularly true for the unclear function of GPER1 in CC, where GPER1 expression may be correlated with both positive (13) and negative (12) prognosis.

Materials and Methods

Cell culture. The human cervical cell lines HeLa (HPV18+), SiHa (HPV16+) and C33-A (HPV−) were obtained from the American Type Cell Collection (ATCC; Manassas, VA, USA) and cultured in minimum essential medium (MEM; L0416-500, Biowest, Nuaillé, France) supplemented with 10% fetal bovine serum (FBS; S181B-500, Biochrom, Berlin, Germany) and 1% Penicillin/Streptomycin (P/S; L0022-100, Biowest). To retain the identity of the cell lines, purchased cells were expanded and aliquots were frozen in liquid nitrogen. A new frozen stock was used every half year and mycoplasma testing of cultured cell lines was performed routinely using the polymerase chain reaction (PCR) Mycoplasma Test Kit I/C (D101-02, Vazyme, Düsseldorf, Germany). All cells were cultured in a humidified atmosphere with 5% CO_2 at 37˚C.

Transfection with GPER1 small interfering ribonucleic acid (siRNA). For reverse transfection of HeLa and SiHa cells, a cell suspension with 147,000 cells/ml was centrifuged and the supernatant was aspirated. Afterwards, the cells were resuspended in a solution with 1.5 ml OptiMEM (31985-062, Gibco by Life Technologies, Carlsbad, CA, USA) per well. Meanwhile, the transfection mix for a 6-well plate, consisting of 500 µl OptiMEM, 3 µl GPER1 siRNA (Sc-60743) or siControl (Sc-37007) (Santa Cruz Biotechnology, Heidelberg, Germany) and 5 µl Invitrogen Lipofectamine RNAiMAX transfection reagent (1377 8150, Thermo Fisher Scientific, Waltham, MA, USA) was vortexed and incubated for 20 min at room temperature. After incubation, the transfection mix was put in the wells with a total amount of 508 µl per well. The cell suspension was carefully added on top. The medium was changed after 6-12 h to normal MEM medium. The cells were either used 24 h after transfection for functional assays or three days after transfection for ribonucleic acid (RNA) isolation. In contrast, a forward transfection method was used for C33-A cells, in which all steps were similar, except that the cells were already seeded in a 6-well plate one day before transfection and on transfection day the medium was changed to OptiMEM. The transfection mix was added on top of the adherent cells.

RNA isolation and complementary deoxyribonucleic acid (cDNA) synthesis. RNA from transfected cells was isolated using the FastGene RNA Basic Kit (FG-80250, Nippon Genetics Europe, Düren, Germany) according to the manufacturer's instructions. RNA samples were diluted to a final concentration of 1 µg of RNA. 2 µl of 60 µM random primer (GeneOn, Ludwigshafen, Germany) and 1 µl deoxyribonucleotide triphosphates (dNTPs) (110-012, GeneOn, Ludwigshafen, Germany) were added to every sample and the RNA was denatured by heating for 5 min to 70˚C. After cooling the samples on ice, 4 µl of 10xM-MuL buffer (M0253L, New England Biolabs, Frankfurt, Germany), 1µl M-MuLVRT reverse transcriptase (M0253L, New England Biolabs), 0.2 µl RNAse inhibitor (105-350, GeneOn) and 4.8 µl of diethyl pyrocarbonate (DEPC) (K028.1, Carl Roth, Karlsruhe, Germany) water [0.1% (v/v) DEPC in deionized water] were added and the mix was gently vortexed. cDNA was synthesized with an incubation step for 5 min at 25˚C, a heating step for an hour at 42˚C and a denaturation step for 20 min at 65˚C. The cDNA was then stored at –20˚C.

Reverse transcription- quantitative PCR (RT-qPCR). cDNA samples were diluted to a concentration of 5 ng/µl with deionized water and 14 µl qPCR mix [2x; 75 mM Tris-HCl (pH 8.8), 20 mM $(NH_4)_2SO_4$, 0.01% Tween 20, 3 mM $MgCl_2$, 0.2 mM dNTPs, 0.25% Triton X-100, 20 U/ml Taq polymerase, 1:40,000 SYBR Green I, 500 mM Trehalose], 9 µl deionized water and 1 µl primer pair mix (10 µM) were added. The CFX Connect Optics module/RT-PCR and the CFX Connect Real-Time system (Bio-Rad Laboratories, Hercules, CA, USA) were used under following conditions: denaturation for 5 min at 95˚C, 95˚C for 10 s, cooling-down to 65˚C for 30 s and heating up to 65-95˚C. Step two and three were repeated 39'. Gene expression was normalized to the housekeeping gene *RPLP0* (forward 5'-GAT TGG CTA CCC AAC TGT TG-3', reverse 5'-CAG GGG CAG CAG CCA CAA A-3') and the samples were quantified based on a standard curve, existing of a 1:4 serial dilution of the cDNA. The primers used were as follows: *CPA4* (forward 5'-TCT GTG TCG GGC ACT GAG TA3', reverse 5'-GAA GCC ATA GGT CCC GGT AT-3'), *FOXL1* (forward 5'-TTT CAA CGC TTC CCT GAT GC-3', reverse 5'-AGA ACC GTG CCA TTG TTT GC-3'), *GPER1* (forward 5'-CCT GCT TCT GTT TCG CGG AT-3', reverse 5'-CAA TGA GGG AGT AGC ACA GGC-3'), *SERPINE1* (forward 5'-ACC CTC AGC ATG TTC ATT GC-3'; reverse 5'-TCA TGT TGC CTT TCC AGT GG-3'), *ZEB1* (forward 5'-GTG ACG CAG TCT GGG TGT AA-3', reverse 5'-TTG CAG TTT GGG CAT TCA TA-3').

Western blot analysis. Cells were lysed in cell lytic M buffer (Sigma, St. Louis, MO, USA) supplemented with 0.1% phosphatase-inhibitor (C2978, Sigma) and 0.1% protease-inhibitor (P5726 and P8340, Sigma). Isolated proteins (40 µg) were fractioned using 12% sodium dodecyl sulfate (SDS) gel and electro-transferred to a polyvinylidene difluoride membrane (IPVH00010, Merck Millipore, Cork, Ireland). Primary antibodies were used against PAI-1 at 1:1,000 dilution (13801-1-AP, Proteintech, Planegg-Martinsried, Germany) and

GAPDH at 1:2,000 dilution (5174S, Cell Signaling, Danvers, MA, USA). The membrane was washed and incubated in horseradish peroxidase-conjugated secondary antibody (NA9340, Amersham, Sigma-Aldrich). Antibody-bond protein bands were assayed using a chemiluminescent luminol enhancer solution (XLS 30100, Cyanagen, Bologna, Italy).

Phalloidin staining. The cells were transfected and grown on round coverslips. After washing with Dulbecco's phosphate buffered saline (DPBS) (P04-36500, PAN-Biotech, Aidenbach, Germany), cells were fixed with 4% perfluoroalkoxy alcane (PFA) (104005.1000, Sigma-Aldrich) at room temperature for 10 min, and permeabilized with Triton X-100 1% (Sigma-Aldrich) in phosphate buffered saline (PBS) for 5 min. After washing steps and blocking with 2% bovine serum albumin (BSA) (8076.2, Carl Rothy) in PBS for 30 min, cells were incubated with Phalloidin for staining the cytoskeleton (1:4,000, Phalloidin CruzFluor^{TM} 555 Conjugate, sc-363794, Santa Cruz Biotechnology, Heidelberg, Germany) and DAPI for staining the nuclei (1:1,000, 4',6-Diamidin-2-phenylindol, NBP2-31156, Novus Biologicals, Centennial, CO, USA) for 30 min in the dark. Coverslips were mounted with Mowiol (81381, Sigma-Aldrich) and analyzed with ImageJ 1.52a.

Immunofluorescence staining tumor spheres. 1,000 cells per well were seeded on a Nexcelom ULA-96U, ultra-low attachment treated plate (Nexcelom Bioscience, Lawrence, KS, USA) and incubated for 48 h. 50 µl of cooled Matrigel (354234, Corning Life Sciences, Tewksburry, MA, USA) was added and after a short centrifugation, the plate was incubated for nine days. Then, the plate was stored on ice for 20 min to liquify the Matrigel and after that, the tumor spheres were gently transferred to a x-well cell culture chamber with 8-wells on PCA slides with removable frames (Sarstedt, Nümbrecht, Germany). After careful washing steps with DPBS, the tumor spheres were fixed for 20 min at room temperature with 3.7% formaldehyde (104005.1000, Sigma-Aldrich Co.) in DPBS. After further washing steps with DPBS, the permeabilization with 1% Triton X-100 (Sigma-Aldrich Co.) in DPBS took place for 10 min. Blocking with 0.5% BSA (8076.2, Carl Roth) in PBS was then performed. After 60 min, the antibody against GPR30 (PA5-28647, GPR30 polyclonal antibody, Invitrogen) with a 1:200 dilution in 0.5% BSA (Carl Roth) in PBS was added to the tumor spheres. The tumor spheres were incubated overnight in the dark under humid conditions at 4˚C. After aspiration of the blocking buffer and washing steps with DPBS, two drops of the secondary antibody [R37118, Alexa Fluor 488 donkey anti-rabbit antibody (secondary) ReadyProbes, Invitrogen] was mixed up with 1ml fluorescence staining solution (2% BSA and 0.25% Triton X-100 in PBS) and 1 µl DAPI (NBP2-31156, 1:1000, 4',6-Diamidin-2-phenylindol, Novus Biologicals). 250 µl of this mixture were added to the tumor spheres and they were incubated for an hour in the dark. After washing, the slides were covered with Dako fluorescence mounting medium (S3023, Dako North America, Carpinteria, CA, USA) and analyzed the day after.

Colony formation assay. 500 and 1,000 cells per well were seeded in a 6-well plate (Greiner Bio-One, Frickenhausen, Germany) one day after transfection. Plates were incubated for at least seven days. As soon as colonies emerged, the plate was stained with crystal violet, photographed using the CeligoS Cell Imaging Cytometer (Nexcelom Bioscience LLC) and analyzed with ImageJ 1.52a.

Proliferation assay. The day after transfection, 2,000 cells per well were seeded in a 96-well plate and incubated for at least six days. Starting with the seeding day (day 0), the wells were photographed, and confluency was analyzed every 48 h with the CeligoS Cell Imaging Cytometer (Nexcelom Bioscience LLC).

Tumor sphere formation assay. The day after transfection, 500 and 1,000 cells per well were seeded in a 96-well ultra-low attachment plate with flat bottom. Beginning with day five after transfection, the wells were photographed every 96 h until day 17 after transfection. The tumor spheres were analyzed with ImageJ.

Tumor sphere formation assay with Matrigel. The day after transfection, 1,000 cells per well were seeded in a Nexcelom ULA-96U, ultra-low attachment treated plate and incubated for 48 h. Then, 50 µl of Matrigel (354234, Corning Life Sciences) were added and the plate was centrifuged at 300 G for 3 min at 4˚C. The day of Matrigel addition was defined as day 0 and the wells were photographed with the CeligoS Cell Imaging Cytometer (Nexcelom Bioscience LLC). The tumor spheres were analyzed with ImageJ.

Statistical analysis and graph design. Data was statistically analyzed with *t*-tests and Mann-Whitney *U*-tests using GraphPad Prism 8.0.1. Whenever the two-tailed *t*-test just missed significance, we performed the one-tailed *t*-test. The one-tailed *t*-test has a higher power to detect an effect in a particular direction. This is appropriate because an effect in the untested direction was not expected. All experiments were performed in at least biological triplicates and technical duplicates or triplicates.

Results

In all assays with GPER1 knockdown described in this work, GPER1 knockdown was carried out in HeLa and SiHa cells by reverse transfection. Because of their sensitivity, GPER1 knockdown in C33-A cells was performed by forward transfection.

Confirmation of successful knockdown of GPER1 in cervical carcinoma cells using RT-qPCR. Following GPER1 knockdown, RNA was isolated, cDNA synthesized and RT-qPCR was carried out for the quantification of the expression of *GPER1* and the housekeeping gene *RPLP0*. Relative gene expression of *GPER1* in HeLa cells (Figure 1A) of the GPER1 knockdown group (M=0.31, SD=0.06, SEM=0.03) compared to the control group (M=1.00, SD=0.05, SEM=0.03) was significantly lower (p=0.0001). The relative gene expression of *GPER1* in the C33-A (Figure 1B) GPER1 knockdown group (M=0.54; SD=0.29; SEM=0.17) compared to the control group (M=1.00; SD=0.18; SEM=0.10) was significantly reduced (p=0.0401). Similarly, the relative gene expression of *GPER1* in SiHa (Figure 1C) GPER1 knockdown group (M=0.45; SD=0.09; SEM=0.05) in comparison to the control group (M=1.00; SD=0.35; SEM=0.20) was also significantly reduced (p=0.0281).

Increased stem cell properties of cervical carcinoma cells by GPER1 knockdown. To investigate the effect of GPER1

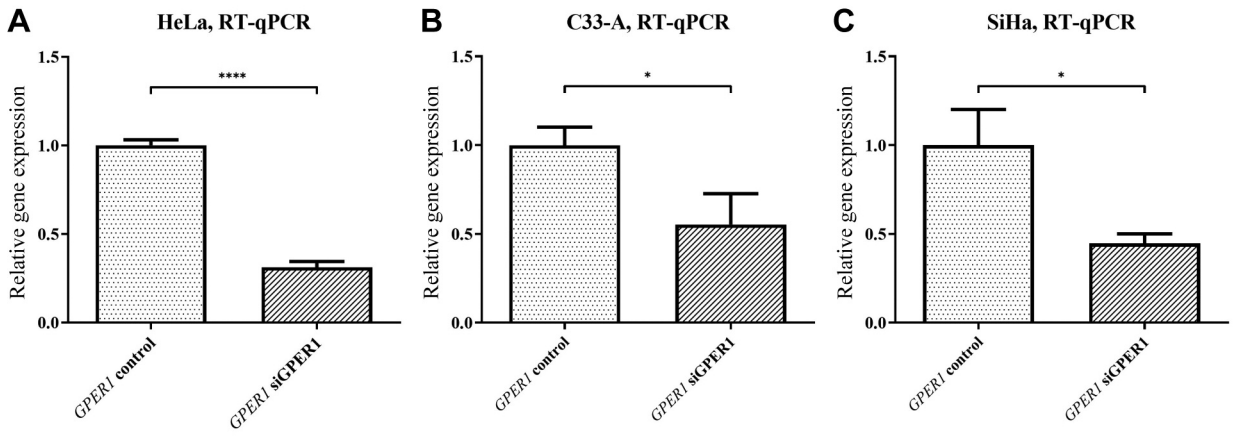

Figure 1. *Successful knockdown of GPER1, measured by RT-qPCR. (A) Significant differences in relative gene expression of GPER1 in the GPER1 knockdown group and in the control group in HeLa, (B) C33-A and (C) SiHa cells. Mean with standard error, n=3, two-tailed t-test in (A), one-tailed t-test in (B, C). Normalized to housekeeping gene RPLP0. *p<0.05 and ****p<0.0001.*

knockdown on stem cell properties, colony formation assays were performed using HeLa, C33-A and SiHa cells. In each case, the size and number of colonies were analyzed. The number of colonies developed from HeLa cells was significantly higher (p=0.0046) in the GPER1 knockdown group (M=156.7; SD=1.53; SEM=0.88) than in the control group (M=130; SD=7.94; SEM=4.58; Figure 2A). There was no significant difference between the GPER1 knockdown group and the control group in colony size (Figure 2B). When comparing the number of colonies developed from C33-A cells (Figure 2C) in the GPER1 knockdown and the control group no significant difference was found. However, there were significantly larger C33-A colonies (p=0.0224) in the GPER1 knockdown group (M=6.68; SD=3.85; SEM=0.34) than in the control group (M=5.68; SD=2.91; SEM=0.27; Figure 2D). The number of colonies developed in SiHa cells was also significantly higher (p=0.0389) in the GPER1 knockdown group (M=165.7; SD=17.01; SEM=9.82) compared to the control group (M=133.3; SD=16.56; SEM=9.56; Figure 2E). Significantly larger (p=0.0002) SiHa colonies were found in the GPER1 knockdown group (M=1.37; SD=0.76; SEM=0.03) compared to the control group (M=1.20; SD=0.59; SEM=0.03; Figure 2F). GPER1 knockdown did not result in increased proliferation. In the GPER1 knockdown group of HeLa cells, even significantly lower proliferation was detectable (data not shown).

Effects of GPER1 knockdown on tumor sphere formation of cervical carcinoma cells. To obtain information about the invasiveness of the cervical carcinoma cells, tumor sphere formation assay was performed using HeLa (Figure 3A, B and Figure 4A, B), C33-A cells (Figure 3C, D and Figure 4C, D) and SiHa cells (Figure 3E, F and Figure 4E, F) with 500 seeded (Figure 4) and 1,000 seeded cells (Figure 3). Firstly, the size of tumor spheres developed from HeLa cells was analyzed (Figure 3A and Figure 4A). At day five, significantly larger HeLa tumor spheres (1,000 cells seeded) (p=0.0041) were detected in the GPER1 knockdown group (Mdn=7577; n=44), compared to the control group (Mdn=3075; n=16; Figure 3A). No significant differences in the size of tumorspheres were measured between the GPER1 knockdown group and the control group on the following nine, thirteen and seventeen days, with 1,000 seeded cells. If 500 HeLa cells were seeded (Figure 4A) there were also significantly larger (p=0.0410) tumorspheres on day five in the GPER1 knockdown group (Mdn=8721; n=54) compared to the control group (Mdn=3816; n=28), but there were no significant differences on the following days.

The average number of tumor spheres of 1,000 seeded HeLa cells (Figure 3B) did not yet show significant differences between the GPER1 knockdown group and the control group on day five, but did from day nine. On this day, significantly more tumor spheres (p=0.0112) were measured in the GPER1 knockdown group (M=5.50; SD=1.87; SEM=0.76), than in the control group (M=3.00; SD=0.63; SEM=0.26). This significant difference increased on day thirteen, at which point the GPER1 knockdown group (M=5.5; SD=1.38; SEM=0.56) has a difference of p=0.0032 compared to the control group (M=2.83; SD=0.98; SEM=0.4). At day seventeen, tumor spheres were also significantly more on average (p=0.0048) in the GPER1 knockdown group (M=4.67; SD=1.21; SEM=0.49) than in the control group (M=2.5; SD=0.84; SEM=0.34).

The average number of tumor spheres with 500 seeded HeLa cells was significantly greater in the GPER1 knockdown group on all measured days (Figure 4B). On day five, the

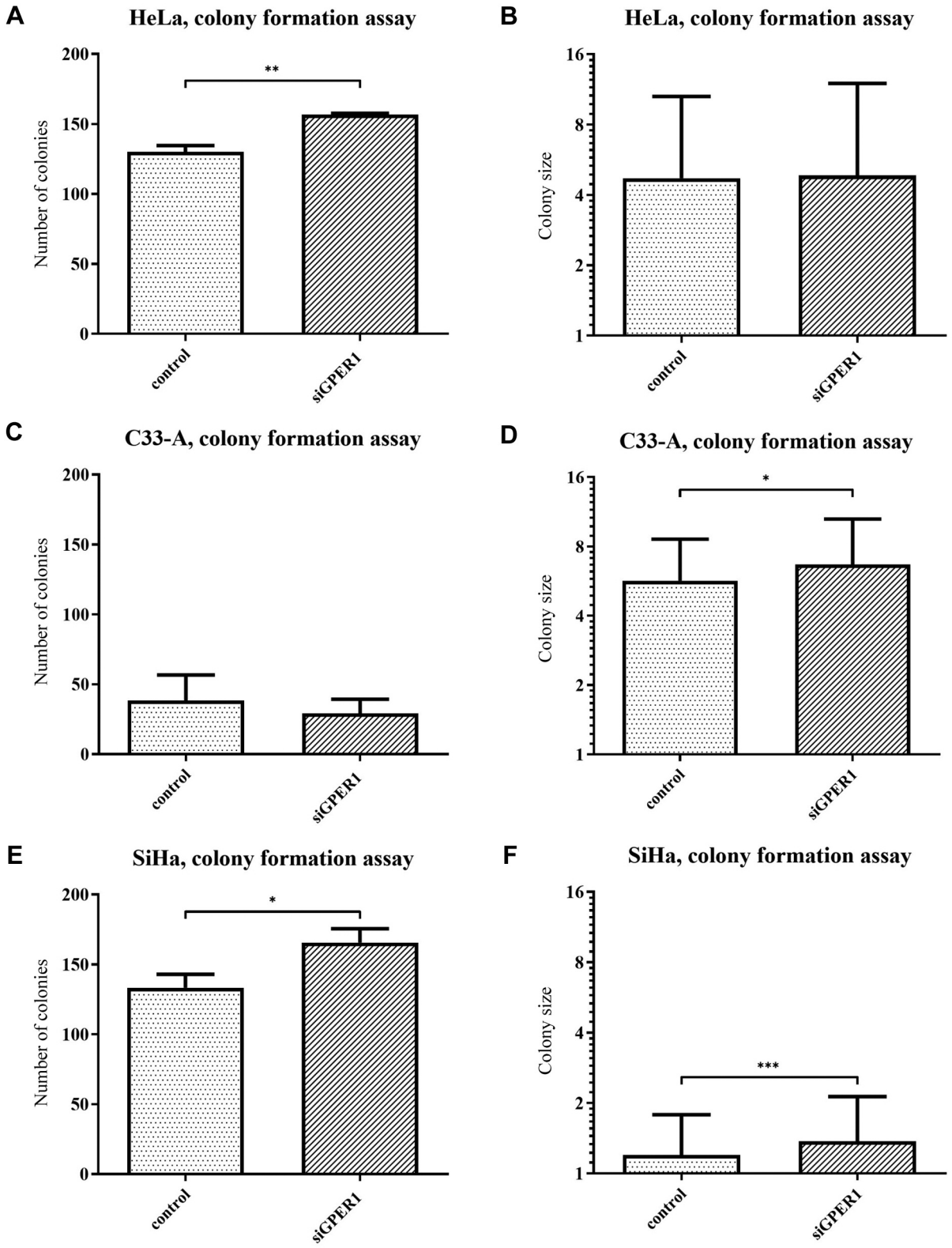

Figure 2. *Colony formation after GPER1 knockdown. Colony formation of HeLa (A, B), C33-A (C, D) and SiHa (E, F) cervical carcinoma cells after knockdown of GPER1 compared with siRNA control. Number of colonies from HeLa (A), C33-A (C) and SiHa (E) cervical carcinoma cells. Size of colonies from HeLa (B), C33-A (D) and SiHa (F) cells. Mean with standard deviation, n=3, two-tailed t-test (A-D, F), one-tailed t-test (E). *p<0.05, **p<0.01 and ***p<0.001.*

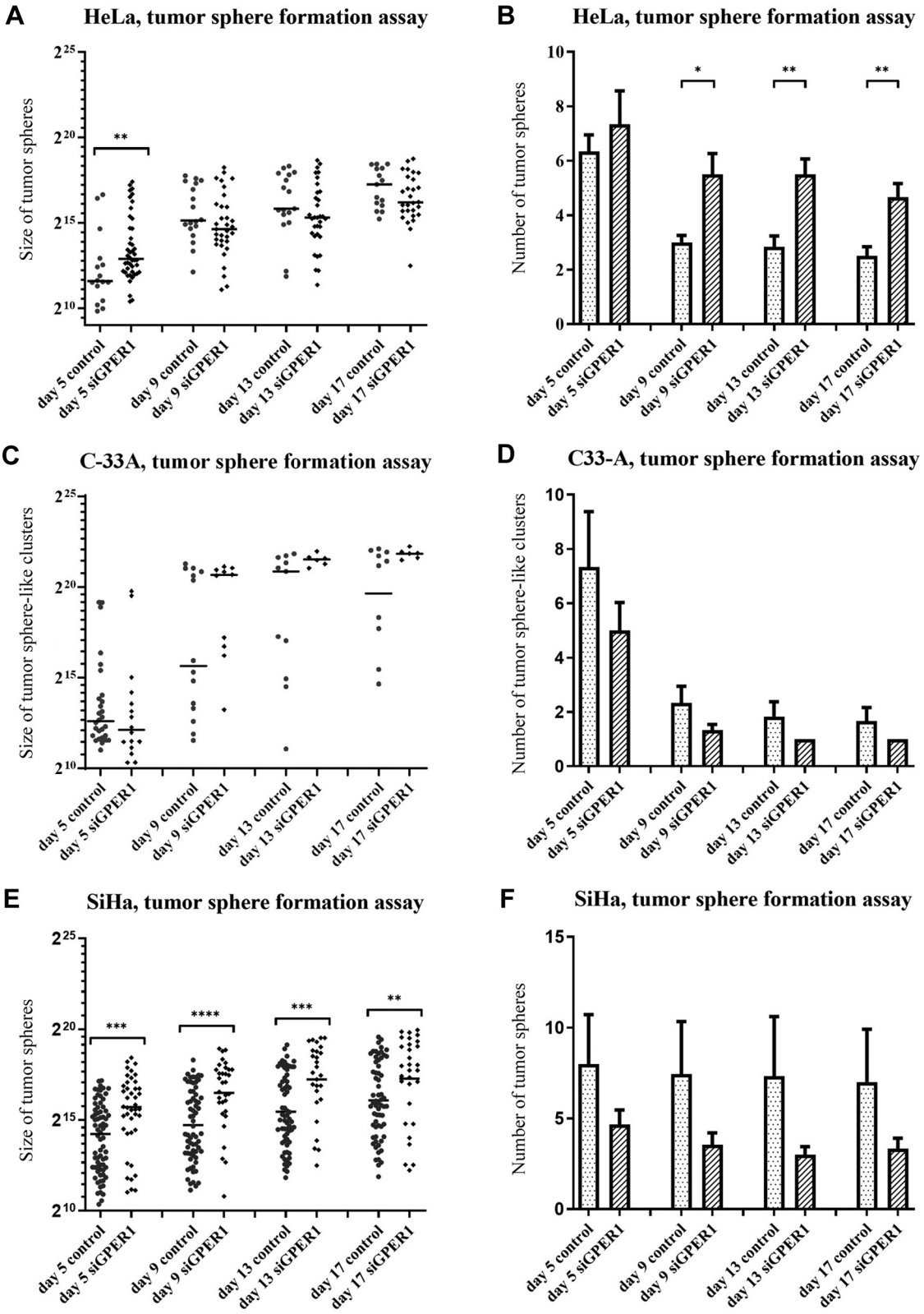

Figure 3. *Tumor sphere formation after GPER1 knockdown. Tumor sphere formation assay with 1000 seeded cells. Size (A, E) and number (B, F) of tumor spheres formed by HeLa (A, B) and SiHa (E, F) cells. Size (C) and number (D) of tumor sphere-like cell clusters formed by C33-A cells. (A, C, E) median, n=3, Mann-Whitney-U test. (B, D, F) mean with standard deviation, n=3, two-tailed t-test. *p<0.05, **p<0.01, ***p<0.001 and ****p<0.0001.*

GPER1 knockdown group (M=9.00; SD=3.46; SEM=1.41) had significantly more tumor spheres compared to the control group (M=4.67; SD=2.50; SEM=1.02) with p=0.0323. On day nine, the difference between the GPER1 knockdown group (M=9.33; SD=3.98; SEM=1.63) and the control group (M=4.50; SD=2.07; SEM=0.85) was significant with p=0.0249. At day thirteen, the significance of the difference (p=0.009) of the GPER1 knockdown group (M=6.00; SD=2.28; SEM=0.93) increased even further compared to the control group (M=2.83; SD=0.75; SEM=0.31). Finally, at day seventeen, the mean number of tumor spheres was also significantly increased in the GPER1 knockdown group (M=6.50; SD=2.35; SEM=0.96) compared to the control group (M=2.83; SD=0.75; SEM=0.31) (p=0.0045).

C33-A cells (Figure 3C, D and Figure 4C, D) did not form solid tumor spheres, but rather tumor sphere-like cell clusters, but these were analyzed similarly to tumor spheres. The size of the tumor sphere-like cell clusters did not show a significant difference neither with 1,000 (Figure 3C) nor with 500 (Figure 4C) seeded C33-A cells on any of the measured days. The number of tumor sphere-like C33-A cell clusters with 1,000 seeded cells (Figure 3D) and with 500 seeded cells (Figure 4D) also did not remain significant across all days.

The analysis of the size of tumor spheres developed from SiHa cells with 1000 seeded cells, showed significantly larger tumorspheres in the GPER1 knockdown group through all measured days (Figure 3E). On day five, significantly larger (p=0.0003) tumorspheres were found in the GPER1 knockdown group (Mdn=53,459; n=42) compared to the control group (Mdn=19,162; n=72). This significant difference in the size of the tumorspheres (p<0.0001) of the GPER1 knockdown group (Mdn=137,540; n=32) compared to the control group (Mdn=19,523; n=67), increased even more on day nine. On day thirteen there were also significantly larger (p=0.0003) tumor spheres in the GPER1 knockdown group (Mdn= 200,102; n=27) compared to the control group (Mdn=36,180; n=66). Finally with the measurement on day seventeen the same significant difference (p=0.0094) by comparing the tumorsphere size of the GPER1 knockdown group (Mdn=238,109; n=30) to the control group (Mdn=61,830; n=63) was shown. If 500 SiHa cells were seeded, the analysis of the size of tumor spheres showed no significant differences between the GPER1 knockdown and the control group across all days (Figure 4E).

SiHa cells showed neither with 1000 (Figure 3F) nor with 500 (Figure 4F) seeded cells significant differences in the number of tumor spheres between the GPER1 knockdown group and the control group.

GPER1 knockdown leads to changed expression of SERPINE1/PAI-1 in cervical carcinoma cells. RT-qPCR was used to analyze expression of *CPA4*, *FOXL1*, *SERPINE1*, *ZEB1* genes after GPER1 knockdown in HeLa cells (Figure 5A). Relative gene expression of *CPA4*, *FOXL1* and *ZEB1* was not significantly changed in the GPER1 knockdown group compared with the control group. *SERPINE1* gene expression was significantly increased (p=0.0343) in the GPER1 knockdown group (M=1.77; SD=0.22; SEM=0.13) compared to the control group (M=1.00; SD=0.36; SEM=0.21). The relative gene expression of *SERPINE1* on C33-A cells (Figure 5B) was decreased (p=0.0417) in the GPER1 knockdown group (M=0.48; SD=0.12; SEM=0.07) compared to the control group (M=1.00; SD=0.38; SEM=0.22). In SiHa cells (Figure 5C) the relative gene expression of *SERPINE1* was not significantly changed in the GPER1 knockdown group compared to the control group.

Subsequently, the expression the *SERPINE1* gene product PAI-1 was checked using Western blot analysis. The relative PAI-1 expression on HeLa cells (Figure 5D, left) was significantly increased (p=0.0270) in the GPER1 knockdown group (M=1.60; SD=0.33; SEM=0.19) compared to the control group (M=1.00; SD=0.20; SEM=0.12). The relative expression of PAI-1 on C33-A cells (Figure 5D, middle) was decreased (p=0.2011) in the GPER1 knockdown group (M=0.37; SD=0.04; SEM=0.03) compared to the control group (M=1.00; SD=0.72; SEM=0.41). However, this difference was not significant. In SiHa cells (Figure 5D, right) the relative expression of PAI-1 was significantly increased (p=0.0242) in the GPER1 knockdown group (M=2.22; SD=0.40; SEM=0.23) compared to the control group (M=1.00; SD=0.44; SEM=0.26).

Effects of GPER1 knockdown on tumor sphere formation of cervical carcinoma cells in Matrigel. To further investigate the invasiveness of HeLa cervical carcinoma cells, a tumor sphere formation assay was performed using Matrigel. Day zero was defined as the day of Matrigel addition, which corresponds to the third day after transfection. We could demonstrate that knockdown of GPER1 expression was significantly effective even on day eight (p=0.0283) with a significant decrease of the relative gene expression of *GPER1* in the GPER1 knockdown group (M=0.51; SD=0.78; SEM=0.06) compared to the control group (M=1.00; SD=0.16; SEM=0.11) (Figure 6A). The main sphere is the largest tumor sphere seen and the subsidiary colonies are smaller colonies that have no contact with the main sphere. Sprouts are cells that extend from the main sphere toward the periphery. For better visualization tumor spheres without (Figure 6B) and with GPER1 knockdown (Figure 6C) were shown. The size of the main spheres was not significantly changed between the two groups on any of the days measured (Figure 6D). The sprouts did not appear until day two. No significant size differences between the GPER1 knockdown group and the control group could be measured over these days (Figure 6E). There was no significant difference in number of sprouts in any of the

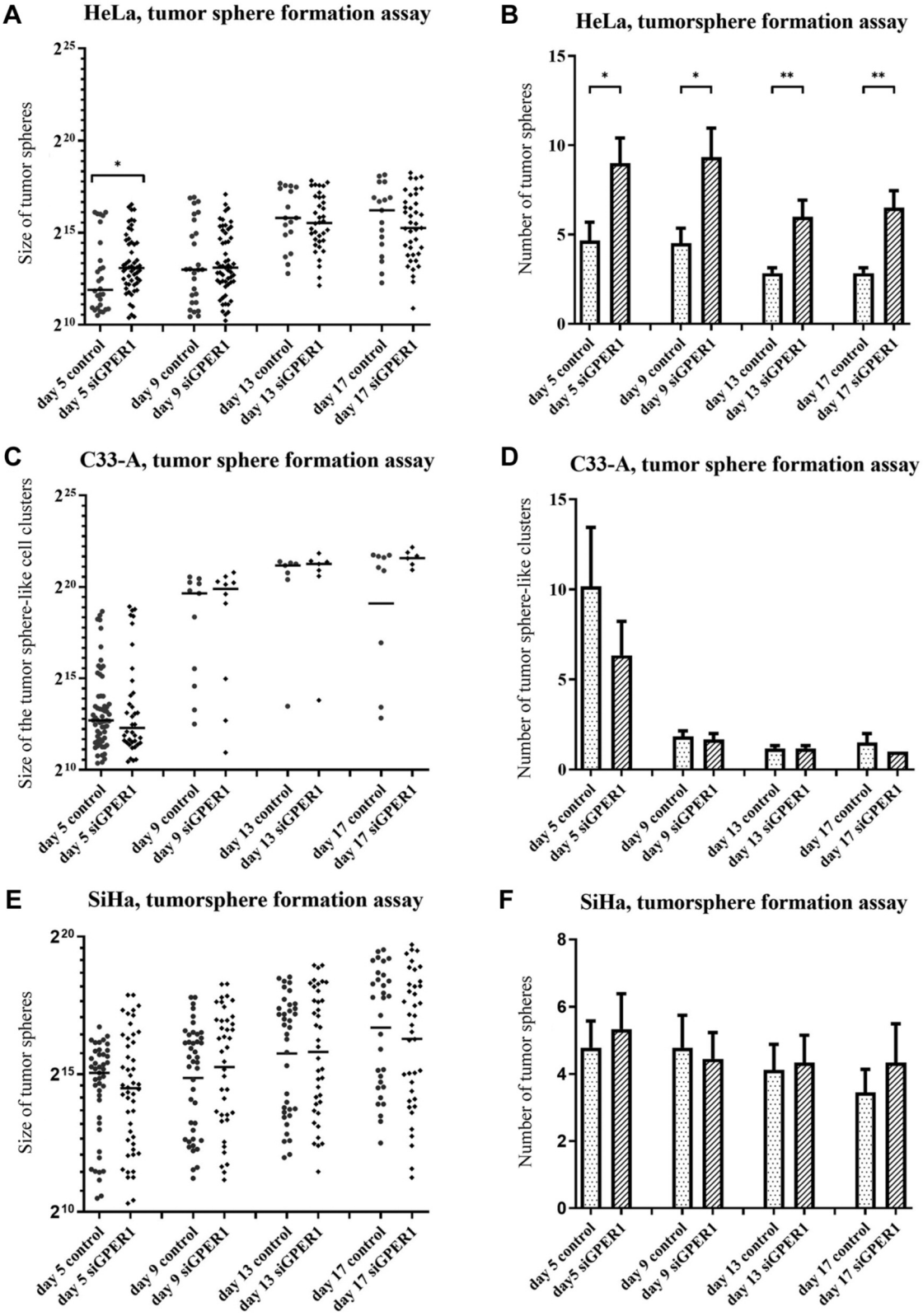

Figure 4. *Tumor sphere formation after GPER1 knockdown. Tumor sphere formation assay with 500 seeded cells. Size (A, E) and number (B, F) of tumor spheres formed by HeLa (A, B) and SiHa (E, F) cells. Size (C) and number (D) of tumor sphere-like cell clusters formed by C33-A cells. (A, C, E) median, n=3, Mann-Whitney-U test. (B, D, F) mean with standard deviation, n=3, two-tailed t-test. *p<0.05 and **p<0.01.*

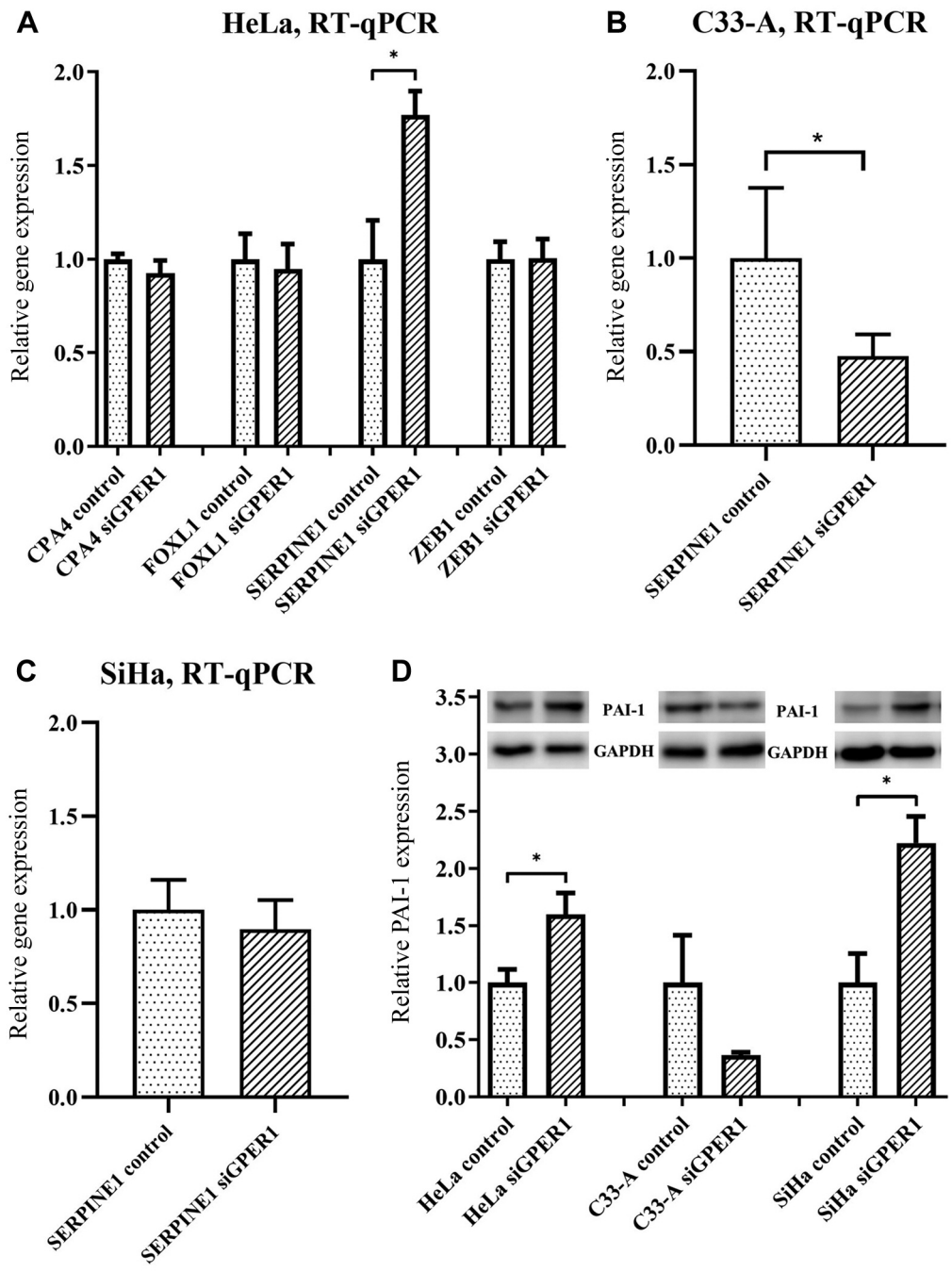

Figure 5. *Relative gene expression of CPA4, FOXL1, SERPINE1, ZEB1 in HeLa cells (A) and SERPINE1 in C33-A (B) and SiHa (C) cells after GPER1 knockdown. Mean with standard error, n=3, two-tailed t-test (A, C) or one-tailed (B). Normalized to RPLP0. Relative expression of SERPINE1 gene product PAI-1 (D) in HeLa, C33-A and SiHa cells after GPER1 knockdown. PAI-1 band intensity was quantified by densitometry and normalized to GAPDH. Mean with standard error, n=3, one-tailed t-test (HeLa), two-tailed t-test (SiHa). *p<0.05.*

measured days (Figure 6F), while the length of the sprouts was not significantly changed on any of the measured days (Figure 6G). Analysis of the size of subsidiary colonies began from day four (Figure 6H). On this day and on day six, the size of the subsidiary colonies of the GPER1 knockdown group were not significantly changed compared to those of the control group. However, on day eight, there were significantly larger subsidiary colonies (p=0.0016) in the GPER1 knockdown group (Mdn=2673; n=523) than in the control group (Mdn=2235; n=494). This significant difference

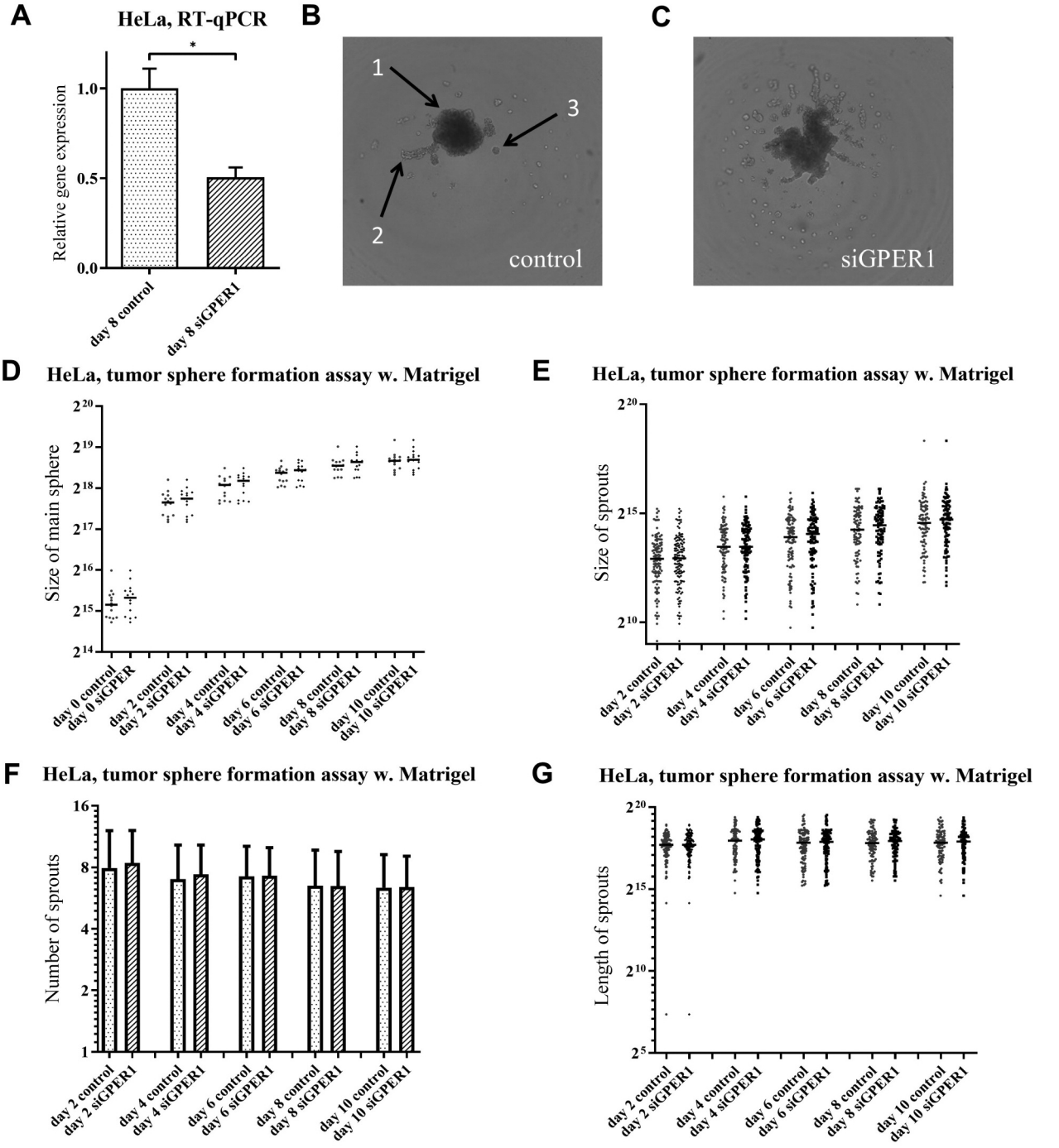

Figure 6. *Continued*

in subsidiary colony size between the GPER1 knockdown group (Mdn=4048; p=519) and the control group (Mdn=3492; n=523) increased further on day ten (U=117492; p=0.0002). The average number of subsidiary colonies did not remain significantly changed across all days (Figure 6I).

Morphological changes after GPER1 knockdown in cervical carcinoma cells. To study cell morphology, HeLa cells were stained with DAPI and phalloidin (Figure 7). The morphology of the cells was analyzed by the ratio of length to width (Figure 7C). The cells from the GPER1 knockdown group (Mdn=2,883;

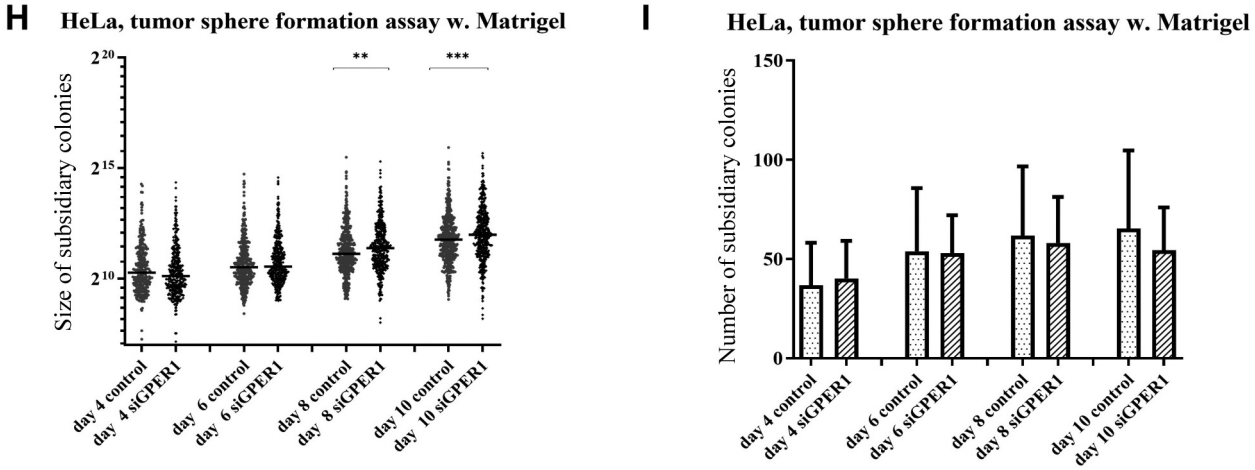

Figure 6. *Tumor sphere formation in Matrigel after GPER1 knockdown in tumor spheres developed from HeLa cervical carcinoma cells. Day 3 after transfection is defined as day 0. The main sphere is the largest tumor sphere forming from day 0. Sprouts start from main sphere to periphery. Subsidiary colonies are smaller colonies formed without contact with a main sphere. Evidence of successful knockdown of GPER1 on day eight using qPCR. Relative gene expression of GPER1 in HeLa cells after GPER1 knockdown. (A). Control spheroid (B): arrow 1 = main sphere, arrow 2 = sprouts, arrow 3 = subsidiary colonies; spheroid after GPER1 knockdown (C). Size of main sphere (D), size of sprouts (E), number of sprouts (F), length of sprouts (G), size of subsidiary colonies (H), number of subsidiary colonies (I). Mean with standard error, n=2, one-tailed t-test, normalized to RPLP0 (A). Median, n=3, Mann-Whitney U test (D, E, G, H). Mean with standard error, n=3, two-tailed t-tests (F, I). *p<0.05, **p<0.01 and ***p<0.001.*

n=133) had a significantly larger length to width ratio (*p*=0.0119) than those from the control group (Mdn=2,338; *n*=138). Thus, they were longer and narrower on average than those of the control group. The filopodia of the cells were analyzed in their length (Figure 7D) and number (Figure 7E). The filopodia from the GPER1 knockdown group (M=267.1; SD=32.99; SEM=19.05) were significantly longer (*p*=0.0169) than those of the control group (M=181.4; SD=18.03; SEM=10.41). The average number of filopodia in the GPER1 knockdown group was similar to that of cells in the control group.

Localization of GPER1 in tumor spheres of cervical carcinoma cells. To localize GPER1 within the tumor spheres, HeLa tumor spheres were grown in Matrigel, GPER1 was stained by immunofluorescence, fixed on slides and analyzed under an Olympus IX83 microscope using the CellSensDimension software (Olympus Europe, Hamburg, Germany). Biological triplicates, each with a control staining without anti-GPER1 antibody but with DAPI and the secondary antibody, and three to four stainings with anti-GPER1 antibody per cell passage were performed. In all tumor spheres examined with anti-GPER1 antibody, there was a marked increase in localization of GPER1 in the periphery and sprouts of the tumor spheres (Figure 7F).

Discussion

As an important ubiquitous receptor that is responsible for rapid estrogen-induced effects *via* various signaling cascades (9), the role of GPER1 in cervical carcinoma has been poorly studied. The current state of research is largely based on studies in breast carcinoma. In various cancer entities, GPER1 appears to play tumor suppressive as well as tumor supportive roles (9). Interestingly, this diversity exists even within the same tumor entity (15). The purpose of this work was therefore to find out how GPER1 behaves in cervical carcinoma.

To gain initial insight into the stem cell properties of the cells, a colony formation assay was performed using HeLa, C33-A and SiHa CC cells. Stem cell properties of tumor cells are a large factor in why tumors metastasize and recur (16). In MCF-7 breast cancer cells, it was found that under estrogen administration, GPER1 led to increased formation of colonies (17), which is contrary to the results shown in cervical carcinoma cells in this work. Here, analysis of the number and size of colonies revealed that there was an increased number of colonies in HeLa and an increased size of colonies in C33-A cells in the GPER1 knockdown group. In SiHa cells both the number and the size of the colonies were increased. It is this difference in the behavior of different tumor entities that shows the relevance of learning more about the role of GPER1 in CC. The colony formation assay shows the ability of a single cell to grow into a colony and thus represents stem cell characteristics. Measurement of colony size provides additional information. Long-lasting promotion of cell proliferation can be observed based on increased colony size. Consequently, the findings of the colony formation assays performed in this work lead to the conclusion that GPER1 seems to have an inhibitory effect on

stem cell properties of HeLa and SiHa cervical carcinoma cells and, thus, suppresses the degenerative behavior of the tumor. However, further research is needed to confirm the inhibition of stem cell properties. In contrast, in C33A cells, GPER1 seems to affect mainly cell growth, as it only affected colony size.

In ovarian cancer cells, activation of GPER1 by its agonist G-1 resulted in decreased proliferation (18). This fits with a study showing that GPER1 expression is significantly lower in ovarian cancer than in benign and low-grade malignant ovarian tumors. Additionally, GPER-1 expression correlated with favorable clinical outcome in ovarian cancer (19). Also in renal cell carcinoma, activation of GPER1 with the GPER1 agonist G1 has shown an antitumor activity (20). However, a study of GPER1 in breast carcinoma showed that cells treated with tamoxifen, which is an agonist on GPER1, had significantly greater proliferation compared with the control group (21). Furthermore, in triple-negative breast carcinoma cells, GPER1 knockdown appeared to result in decreased cell growth (22). Another study showed that knockdown of GPER1 reduced the metastatic behavior of triple-negative breast carcinoma cells, improved the anti-invasive efficacy of selective ERβ agonists, and sensitized the cells to 4OH-tamoxifen (23). Based on these diverse findings, the question arose as to how cervical carcinoma cells change in their proliferative behavior, as a result of GPER1 knockdown. In cervical carcinoma cells, no increased proliferation was detectable in the appropriate GPER1 knockdown groups. However, significantly less proliferation was found in HeLa cells in the GPER1 knockdown group. Opposite effects on proliferation of different cell lines of one tumor entity were also described by Hernández-Silva *et al*. (9) with regards to the ovarian cancer cell lines OVCAR5 and SKOV-3, among others. In OVCAR5 cells, activation of GPER1 by G-1 seems to lead to increased proliferation and in SKOV-3 cells to decreased proliferation (9). The reason why there is significantly decreased proliferation in HeLa cells with GPER1 knockdown could perhaps underlie activation of possibly other proliferation-inhibiting signaling cascades triggered by GPER1 knockdown. For example, the transcription factor *FOXO3a* inhibits proliferation in breast carcinomas (24). GPER1, in turn, induces degradation of *FOXO3a via* EGF-R (25). However, if *FOXO3a* is degraded less in GPER1 knockdown cells, more *FOXO3a* is present in the nucleus, and this could lead to increased suppression of proliferation. This could be an explanation for the significant difference in relative confluence between the GPER1 knockdown and control groups in HeLa cells. On the other hand, it was shown that activation of GPER1 by G-1 leads to decreased proliferation in cervical carcinoma cells (14).

The ability of single cells to form tumor spheres reveals other properties of stem cells that are indispensable for the subsequent metastasis of tumors in the human body (26). Here, on day five, HeLa cells showed significantly larger tumor spheres in the GPER1 knockdown group compared to the control group, further suggesting a tumor suppressive effect of GPER1 in cervical carcinoma cells. However, from day five, a stagnation in the growth of tumor spheres in the GPER1 knockdown group, to a shift to larger tumor spheres in the control group, was observed. One explanation for this behavior could be, on the one hand, that GPER1 knockdown is no longer effective from day five and therefore the cells are inhibited in their further tumor growth by GPER1. To test this, the relative gene expression of GPER1 in GPER1 knockdown cells was measured by qPCR and compared with that of the control group. This was still significantly decreased in the GPER1 knockdown group even at day eight. Therefore, this cause can be excluded. A second cause could be that the cells of the control group grow steadily, but due to the lack of tumor suppressive effect of GPER1 in the GPER1 knockdown group, there is an activation of other tumor suppressive factors after a few days, which influence the growth behavior of the tumor spheres. On one hand, this could be an activation of a tumor suppressor that attenuates further growth; on the other hand, apoptosis or autophagy inducing factors could lead to reduced growth. Kindlin-2 appears to positively influence cell autophagy *via* inhibition of the AKT/mTOR pathway, leading to reduced migration behavior (27). GPER1 also stimulates Akt *via* EGF-R and PI3K. Possibly, there could be a link here by which lack of GPER1 leads to increased activity of Kindlin-2 or decreased activity of the Akt/mTOR pathway and thus slowed tumor sphere growth. However, the number of tumor spheres was significantly greater in the GPER1 knockdown group compared to the control group across all days. Thus, there was increased migration and invasion behavior of HeLa cells with GPER1 knockdown in this assay.

SiHa cells showed significantly larger tumor spheres in the GPER1 knockdown group compared to the control group across all days. However, the number of tumor spheres in the GPER1 knockdown group was tendentially but not significantly reduced. C33-A cells did not form tumor spheres true to definition, which is why they are called tumor sphere-like cell clusters in this work. A tumor sphere is characterized by the fact that it is not possible to discern individual cells in the tumor sphere (28). However, this is exactly what was possible with C33-A cells. In general, they showed a different behavior than HeLa cells, but without significant differences between the GPER1 knockdown group and the control group. The tumor sphere-like cell clusters of the GPER1 knockdown group tended to be larger than those of the control group on some days, but smaller in number on all days. This partly contrary behavior of the C33-A cells compared with that of HeLa cells could be attributed to the lack of formation of stable tumor spheres. The tumor sphere-like cell clusters of the C33-A cells appeared

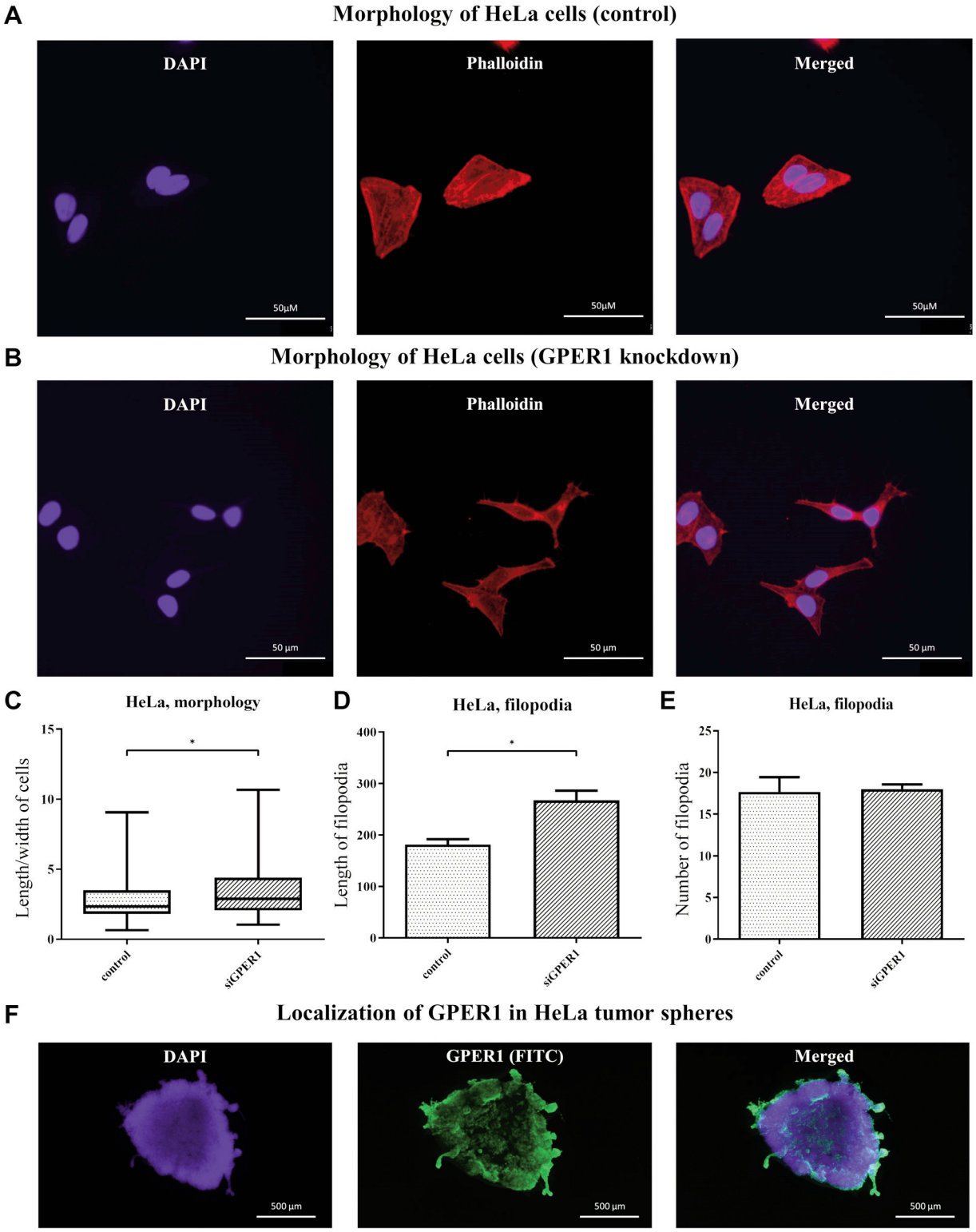

Figure 7. *Morphological changes after GPER1 knockdown in HeLa cervical carcinoma cells. Control group (A) and GPER1 knockdown group (B) stained with DAPI (blue) and Phalloidin (red). Length/width ratio of the cells (C), length of filopodia (D), number of filopodia (E). Median, n=3, Mann-Whitney U test (C), mean with standard error, n=3, two-tailed t-test (D, E). *p<0.05. (F) Localization of GPER1 in tumor spheres developed from HeLa cervical carcinoma cells. HeLa cell tumor spheres stained with DAPI (blue) and anti GPER1 antibody (green). DAPI (left), GPER1 (middle) and combination of both (right).*

much more unstable than tumor spheres of the HeLa cells, making a concrete comparison between C33-A and HeLa cells in terms of tumor sphere growth difficult. Establishing a functional knockdown was also more difficult with C33-A cells, as the majority of these did not survive reverse transfection.

The unique feature of the tumor sphere formation assay with Matrigel is that it does not allow the cells to adhere to the bottom of the well plate. Matrigel also prevents the tumor spheres from moving freely and fusing with other tumor spheres (26). The size of the main spheres of HeLa cells showed no significant difference between the GPER1 knockdown group and the control group, but a slight tendency towards larger main spheres in the GPER1 knockdown group. The same was seen for the size of the sprouts. In addition, there was a significant difference in the size of the subsidiary colonies. The subsidiary colonies of the GPER1 knockdown group were significantly larger than those of the control group on day eight and ten. This suggests a higher invasiveness of the cells with reduced GPER1 expression, since if hypothetically applied to the human body, the subsidiary colonies would behave like metastases. However, when GPER1 is considered in other systems, opposite behavior has been observed; gastric cancer cells lacking GPER1 appear to exhibit less invasion and migration behavior (29). However, according to the evidence found in this work by the tumor sphere formation assay using Matrigel, the increased size of the subsidiary colony size of the GPER1 knockdown group suggests that GPER1 knockdown in CC cells leads to increased invasive behavior.

After GPER1 knockdown, there was a significant increase in the relative gene expression of *SERPINE1* in HeLa cells. The gene product of *SERPINE1*, also referred to as PAI-1, is a plasminogen activator inhibitor, meaning that the degradation of fibrin is inhibited by the *SERPINE1* gene product, among other factors (30), was also increased. In addition, *SERPINE1* induces angiogenesis and plays a role in cell mobility and extracellular matrix homeostasis. In cervical carcinomas, an association between *SERPINE1* and poor overall or disease-free survival has been found (31). *SERPINE1* is expressed in many tumors and shows worse overall survival in breast carcinomas, among others. Increased tumor metastasis and poor response to chemotherapy in breast carcinomas also appear to be attributable to *SERPINE1* (30). Thus, if GPER1 is decreased by knockdown, the gene and protein expression of *SERPINE1* in HeLa cells is significantly increased compared to the control group. A conclusion of this would be that in HeLa cells GPER1 inhibits the expression of *SERPINE1* and consequently its suppression increases it. This further confirmed the hypothesis that GPER1 has a tumor suppressive effect in HeLa cervical carcinoma cells. In SiHa cells, *SERPINE1* gene expression remained unchanged after GPER1 knockdown whereas expression of the *SERPINE1* gene product PAI-1 was also increased. The decrease in *SERPINE1* gene and protein expression in C33-A cells after GPER1 knockdown is interesting, especially since these cells did not show significant tumor sphere formation. It is striking that *SERPINE1*/PAI-1 is downregulated in an HPV-negative CC cell line. However, we cannot say whether there is a correlation here. For this, further HPV-positive, as well as HPV-negative CC cell lines have to be compared.

While comparing the GPER1 knockdown group and the control group, the relative gene expression of FOXL1 and ZEB1 showed no significant changes. FOXL1 has tumor suppressive effects in breast cancer (32), and a negative prognosis was noted for patients with CC when ZEB1 was increased (33). However, based on our results a GPER1 knockdown does not influence the expression of FOXL1 and ZEB1 in any direction.

Epithelial-mesenchymal transition (EMT) refers to the transition from epithelial to mesenchymal cells. These mesenchymal cells are able to move through the extracellular matrix and, in contrast to epithelial cells, have spindle-shaped cell bodies with pseudo- or filopodia. All of this is for cell motion, invasiveness and metastasis of the tumor (34). In a study on breast carcinomas, it was found that inhibition of GPER1 by its antagonist G15 resulted in decreased EMT (35). The morphology of HeLa cells clearly changed after GPER1 knockdown. The cells in the GPER1 knockdown group had more stress fibers and a larger length-to-width ratio than cells of the control group. Spindle-shaped cells are more likely to be mesenchymal (34), which means that after knockdown of GPER1, EMT seems to be increased in cervical carcinoma cells. Further evidence for this was provided by analysis of the cells' filopodia. Filopodia are protrusions of the cell membrane (36) that contain actin and are thus able to support cell motility and tumor metastasis (37). While the cells in the GPER1 knockdown group had approximately the same average number of filopodia as the cells in the control group, they had significantly longer filopodia. Thus, the cells with GPER1 knockdown showed mesenchymal features with longer filopodia than those of the control group, which appeared more epithelial. GPER1 knockdown may lead to increased EMT in cervical carcinoma cells, and therefore GPER1 appears to have a tumor suppressive effect. To make more precise statements, further studies on mesenchymal markers and morphology are necessary.

To learn more about the role of GPER1 in cervical carcinoma, it is interesting to find out where GPER1 in its physiological form is localized in the tumor sphere. Using immunofluorescence, GPER1 was shown to be localized more in the sprouts and peripheral portions of the tumor sphere. A tumor sphere can be divided into three areas, which, starting from the center of the tumor sphere, represent the necrotic, the quiescent and the proliferating zone. The quiescent zone contains quiescent cells, which are not in their proliferating

phase (38). Since GPER1 was mainly detected in the peripheral areas and the sprouts of the tumor spheres, GPER1 seems to be more abundant in the proliferative zone, accordingly in the invasive front of the tumor. In order to support this, the fluorescence signal along the axes of the spheres must be evaluated in further investigations.

Conclusion

GPER1 appears to have a tumor suppressive role in cervical carcinoma, as GPER1 knockdown provoked increased stem cell properties in colony formation assay as well as increased invasive behavior in tumor spheres formation assay. Furthermore, there was an increased expression of the oncogene *SERPINE1* due to GPER1 knockdown. Epithelial-mesenchymal transition also appears to be enhanced in cells of reduced GPER1 expression. The findings of this work form a basis for further research and contribute to a better understanding of the disease. In addition, for further studies and especially for therapeutic application, it is important to develop new, effective agents, agonists as well as antagonists. It should be noted that the efficacy exclusively at GPER1 is strongly dependent on their chemical structure (39). On the other hand, substances are also needed that do not act at GPER1 but can be used, for example, in the treatment of menopausal problems (39).

Conflicts of Interest

The Authors declare no conflicts of interest in relation to this study.

Authors' Contributions

Conceptualization: Carsten Gründker; Investigation: Sophia Ruckriegl, Johanna Loris and Katsiaryna Wert; Project administration: Carsten Gründker; Writing - original draft: Carsten Gründker and Sophia Ruckriegl; Writing - review & editing: Gerd Bauerschmitz and Julia Gallwas.

Acknowledgements

The Authors thank Sonja Blume for excellent technical assistance.

References

1 Sung H, Ferlay J, Siegel RL, Laversanne M, Soerjomataram I, Jemal A and Bray F: Global cancer statistics 2020: GLOBOCAN estimates of incidence and mortality worldwide for 36 cancers in 185 countries. CA Cancer J Clin *71(3)*: 209-249, 2021. PMID: 33538338. DOI: 10.3322/caac.21660

2 Läsche M, Gallwas J and Gründker C: Like brothers in arms: How hormonal stimuli and changes in the metabolism signaling cooperate, leading HPV infection to drive the onset of cervical cancer. Int J Mol Sci *23(9)*: 5050, 2022. PMID: 35563441. DOI: 10.3390/ijms23095050

3 Läsche M, Urban H, Gallwas J and Gründker C: HPV and other microbiota; who's good and who's bad: Effects of the microbial environment on the development of cervical cancer-A non-systematic review. Cells *10(3)*: 714, 2021. PMID: 33807087. DOI: 10.3390/cells10030714

4 Bosch FX, Lorincz A, Muñoz N, Meijer CJ and Shah KV: The causal relation between human papillomavirus and cervical cancer. J Clin Pathol *55(4)*: 244-265, 2002. PMID: 11919208. DOI: 10.1136/jcp.55.4.244

5 Beckmann MW, Stübs FA, Koch MC, Mallmann P, Dannecker C, Dietl A, Sevnina A, Mergel F, Lotz L, Hack CC, Ehret A, Gantert D, Martignoni F, Cieslik JP, Menke J, Ortmann O, Stromberger C, Oechsle K, Hornemann B, Mumm F, Grimm C, Sturdza A, Wight E, Loessl K, Golatta M, Hagen V, Dauelsberg T, Diel I, Münstedt K, Merz E, Vordermark D, Lindel K, Wittekind C, Küppers V, Lellé R, Neis K, Griesser H, Pöschel B, Steiner M, Freitag U, Gilster T, Schmittel A, Friedrich M, Haase H, Gebhardt M, Kiesel L, Reinhardt M, Kreißl M, Kloke M, Horn LC, Wiedemann R, Marnitz S, Letsch A, Zraik I, Mangold B, Möckel J, Alt C, Wimberger P, Hillemanns P, Paradies K, Mustea A, Denschlag D, Henscher U, Tholen R, Wesselmann S and Fehm T: Diagnosis, therapy and follow-up of cervical cancer. Guideline of the DGGG, DKG and DKH (S3-Level, AWMF Registry No. 032/033OL, May 2021) - Part 1 with recommendations on epidemiology, screening, diagnostics and therapy. Geburtshilfe Frauenheilkd *82(2)*: 139-180, 2022. PMID: 35169387. DOI: 10.1055/a-1671-2158

6 Fehm T, Stübs FA, Koch MC, Mallmann P, Dannecker C, Dietl A, Sevnina A, Mergel F, Lotz L, Carolin C.Hack, Ehret A, Gantert D, Martignoni F, Cieslik JP, Menke J, Ortmann O, Stromberger C, Oechsle K, Hornemann B, Mumm F, Grimm C, Sturdza A, Wight E, Loessl K, Golatta M, Hagen V, Dauelsberg T, Diel I, Münstedt K, Merz E, Vordermark D, Lindel K, Wittekind C, Küppers V, Lellé R, Neis K, Griesser H, Pöschel B, Steiner M, Freitag U, Gilster T, Schmittel A, Friedrich M, Haase H, Gebhardt M, Kiesel L, Reinhardt M, Kreißl M, Kloke M, Horn LC, Wiedemann R, Marnitz S, Letsch A, Zraik I, Mangold B, Möckel J, Alt C, Wimberger P, Hillemanns P, Paradies K, Mustea A, Denschlag D, Henscher U, Tholen R, Wesselmann S and Beckmann MW: Diagnosis, therapy and follow-up of cervical cancer. Guideline of the DGGG, DKG and DKH (S3-Level, AWMF Registry No. 032/033OL, May 2021) - Part 2 with recommendations on psycho-oncology, rehabilitation, follow-up, recurrence, palliative therapy and healthcare facilities. Geburtshilfe Frauenheilkd *82(2)*: 181-205, 2022. PMID: 35197803. DOI: 10.1055/a-1671-2446

7 de la Garza-Salazar JG, Meneses-Garcia A and Morales-Vásquez F: Cervical cancer. Berlin, Germany, Springer, 2017.

8 Prossnitz ER and Barton M: Estrogen biology: new insights into GPER function and clinical opportunities. Mol Cell Endocrinol *389(1-2)*: 71-83, 2014. PMID: 24530924. DOI: 10.1016/j.mce.2014.02.002

9 Hernández-Silva CD, Villegas-Pineda JC and Pereira-Suárez AL: Expression and role of the G protein-coupled estrogen receptor (GPR30/GPER) in the development and immune response in female reproductive cancers. Front Endocrinol (Lausanne) *11*: 544, 2020. PMID: 32973677. DOI: 10.3389/fendo.2020.00544

10 Bologa CG, Revankar CM, Young SM, Edwards BS, Arterburn JB, Kiselyov AS, Parker MA, Tkachenko SE, Savchuck NP, Sklar LA, Oprea TI and Prossnitz ER: Virtual and biomolecular

screening converge on a selective agonist for GPR30. Nat Chem Biol *2(4)*: 207-212, 2006. PMID: 16520733. DOI: 10.1038/nchembio775

11 Lappano R, Rosano C, De Marco P, De Francesco EM, Pezzi V and Maggiolini M: Estriol acts as a GPR30 antagonist in estrogen receptor-negative breast cancer cells. Mol Cell Endocrinol *320(1-2)*: 162-170, 2010. PMID: 20138962. DOI: 10.1016/j.mce.2010.02.006

12 Ino Y, Akimoto T, Takasawa A, Takasawa K, Aoyama T, Ueda A, Ota M, Magara K, Tagami Y, Murata M, Hasegawa T, Saito T, Sawada N and Osanai M: Elevated expression of G protein-coupled receptor 30 (GPR30) is associated with poor prognosis in patients with uterine cervical adenocarcinoma. Histol Histopathol *35(4)*: 351-359, 2020. PMID: 31483053. DOI: 10.14670/HH-18-157

13 Friese K, Kost B, Vattai A, Marmé F, Kuhn C, Mahner S, Dannecker C, Jeschke U and Heublein S: The G protein-coupled estrogen receptor (GPER/GPR30) may serve as a prognostic marker in early-stage cervical cancer. J Cancer Res Clin Oncol *144(1)*: 13-19, 2018. PMID: 28924735. DOI: 10.1007/s00432-017-2510-7

14 Zhang Q, Wu YZ, Zhang YM, Ji XH and Hao Q: Activation of G-protein coupled estrogen receptor inhibits the proliferation of cervical cancer cells *via* sustained activation of ERK1/2. Cell Biochem Funct *33(3)*: 134-142, 2015. PMID: 25753185. DOI: 10.1002/cbf.3097

15 Arterburn JB and Prossnitz ER: G protein-coupled estrogen receptor GPER: Molecular pharmacology and therapeutic applications. Annu Rev Pharmacol Toxicol *63*: 295-320, 2023. PMID: 36662583. DOI: 10.1146/annurev-pharmtox-031122-121944

16 Huang R and Rofstad EK: Cancer stem cells (CSCs), cervical CSCs and targeted therapies. Oncotarget *8(21)*: 35351-35367, 2017. PMID: 27343550. DOI: 10.18632/oncotarget.10169

17 Yang H, Wang C, Liao H and Wang Q: Activation of GPER by E2 promotes proliferation, invasion and migration of breast cancer cells by regulating the miR-124/CD151 pathway. Oncol Lett *21(6)*: 432, 2021. PMID: 33868470. DOI: 10.3892/ol.2021.12693

18 Han N, Heublein S, Jeschke U, Kuhn C, Hester A, Czogalla B, Mahner S, Rottmann M, Mayr D, Schmoeckel E and Trillsch F: The G-protein-coupled estrogen receptor (GPER) regulates trimethylation of histone H3 at lysine 4 and represses migration and proliferation of ovarian cancer cells *in vitro*. Cells *10(3)*: 619, 2021. PMID: 33799631. DOI: 10.3390/cells10030619

19 Ignatov T, Modl S, Thulig M, Weißenborn C, Treeck O, Ortmann O, Zenclussen A, Costa SD, Kalinski T and Ignatov A: GPER-1 acts as a tumor suppressor in ovarian cancer. J Ovarian Res *6(1)*: 51, 2013. PMID: 23849542. DOI: 10.1186/1757-2215-6-51

20 Chen SK, Wang YC, Lin TY, Wu HJ, Huang CJ and Ku WC: G-protein-coupled estrogen receptor 1 agonist G-1 perturbs sunitinib resistance-related phosphoproteomic signatures in renal cell carcinoma. Cancer Genomics Proteomics *18(3)*: 207-220, 2021. PMID: 33893075. DOI: 10.21873/cgp.20253

21 Molina L, Bustamante F, Ortloff A, Ramos I, Ehrenfeld P and Figueroa CD: Continuous exposure of breast cancer cells to tamoxifen upregulates GPER-1 and increases cell proliferation. Front Endocrinol (Lausanne) *11*: 563165, 2020. PMID: 33117280. DOI: 10.3389/fendo.2020.563165

22 Girgert R, Emons G and Gründker C: Inactivation of GPR30 reduces growth of triple-negative breast cancer cells: possible application in targeted therapy. Breast Cancer Res Treat *134(1)*: 199-205, 2012. PMID: 22290080. DOI: 10.1007/s10549-012-1968-x

23 Schmitz V, Bauerschmitz G, Gallwas J and Gründker C: Suppression of G protein-coupled estrogen receptor 1 (GPER1) enhances the anti-invasive efficacy of selective ERβ agonists. Anticancer Res *42(11)*: 5187-5194, 2022. PMID: 36288854. DOI: 10.21873/anticanres.16025

24 Zou Y, Tsai WB, Cheng CJ, Hsu C, Chung YM, Li PC, Lin SH and Hu MC: Forkhead box transcription factor FOXO3a suppresses estrogen-dependent breast cancer cell proliferation and tumorigenesis. Breast Cancer Res *10(1)*: R21, 2008. PMID: 18312651. DOI: 10.1186/bcr1872

25 Girgert R, Emons G and Gründker C: Estrogen signaling in ERα-negative breast cancer: ERβ and GPER. Front Endocrinol (Lausanne) *9*: 781, 2019. PMID: 30687231. DOI: 10.3389/fendo.2018.00781

26 Bahmad HF, Cheaito K, Chalhoub RM, Hadadeh O, Monzer A, Ballout F, El-Hajj A, Mukherji D, Liu YN, Daoud G and Abou-Kheir W: Sphere-formation assay: Three-dimensional *in vitro* culturing of prostate cancer stem/progenitor sphere-forming cells. Front Oncol *8*: 347, 2018. PMID: 30211124. DOI: 10.3389/fonc.2018.00347

27 Wu G, Long Y, Lu Y, Feng Y, Yang X, Xu X and Yao D: Kindlin 2 suppresses cervical cancer cell migration through AKT/mTOR mediated autophagy induction. Oncol Rep *44(1)*: 69-76, 2020. PMID: 32377753. DOI: 10.3892/or.2020.7603

28 Johnson S, Chen H and Lo PK: *In vitro* tumorsphere formation assays. Bio Protoc *3(3)*: e325, 2013. PMID: 27500184. DOI: 10.21769/bioprotoc.325

29 Xu E, Xia X, Jiang C, Li Z, Yang Z, Zheng C, Wang X, Du S, Miao J, Wang F, Wang Y, Lu X and Guan W: GPER1 silencing suppresses the proliferation, migration, and invasion of gastric cancer cells by inhibiting PI3K/AKT-mediated EMT. Front Cell Dev Biol *8*: 591239, 2020. PMID: 33425895. DOI: 10.3389/fcell.2020.591239

30 McCann JV, Xiao L, Kim DJ, Khan OF, Kowalski PS, Anderson DG, Pecot CV, Azam SH, Parker JS, Tsai YS, Wolberg AS, Turner SD, Tatsumi K, Mackman N and Dudley AC: Endothelial miR-30c suppresses tumor growth *via* inhibition of TGF-β-induced Serpine1. J Clin Invest *129(4)*: 1654-1670, 2019. PMID: 30855280. DOI: 10.1172/JCI123106

31 Hazelbag S, Kenter GG, Gorter A and Fleuren GJ: Prognostic relevance of TGF-beta1 and PAI-1 in cervical cancer. Int J Cancer *112(6)*: 1020-1028, 2004. PMID: 15386352. DOI: 10.1002/ijc.20512

32 Zhong J, Wang H, Yu J, Zhang J and Wang H: Overexpression of Forkhead Box L1 (FOXL1) inhibits the proliferation and invasion of breast cancer cells. Oncol Res *25(6)*: 959-965, 2017. PMID: 27938507. DOI: 10.3727/096504016X14803482769179

33 Chen XJ, Deng YR, Wang ZC, Wei WF, Zhou CF, Zhang YM, Yan RM, Liang LJ, Zhong M, Liang L, Wu S and Wang W: Hypoxia-induced ZEB1 promotes cervical cancer progression *via* CCL8-dependent tumour-associated macrophage recruitment. Cell Death Dis *10(7)*: 508, 2019. PMID: 31263103. DOI: 10.1038/s41419-019-1748-1

34 Yang J and Weinberg RA: Epithelial-mesenchymal transition: at the crossroads of development and tumor metastasis. Dev Cell *14(6)*: 818-829, 2008. PMID: 18539112. DOI: 10.1016/j.devcel.2008.05.009

35 Liu Y, Du FY, Chen W, Fu PF, Yao MY and Zheng SS: G15 sensitizes epithelial breast cancer cells to doxorubicin by

preventing epithelial-mesenchymal transition through inhibition of GPR30. Am J Transl Res *7(5)*: 967-975, 2015. PMID: 26175858.

36 Schaks M, Giannone G and Rottner K: Actin dynamics in cell migration. Essays Biochem *63(5)*: 483-495, 2019. PMID: 31551324. DOI: 10.1042/EBC20190015

37 Machesky LM: Lamellipodia and filopodia in metastasis and invasion. FEBS Lett *582(14)*: 2102-2111, 2008. PMID: 18396168. DOI: 10.1016/j.febslet.2008.03.039

38 Dini S, Binder BJ, Fischer SC, Mattheyer C, Schmitz A, Stelzer EH, Bean NG and Green JE: Identifying the necrotic zone boundary in tumour spheroids with pair-correlation functions. J R Soc Interface *13(123)*: 20160649, 2016. PMID: 27733696. DOI: 10.1098/rsif.2016.0649

39 Segovia-Mendoza M, Mirzaei E, Prado-Garcia H, Miranda LD, Figueroa A and Lemini C: The interplay of GPER1 with 17β-Aminoestrogens in the regulation of the proliferation of cervical and breast cancer cells: a pharmacological approach. Int J Environ Res Public Health *19(19)*: 12361, 2022. PMID: 36231664. DOI: 10.3390/ijerph191912361

Received February 16, 2023
Revised March 2, 2023
Accepted March 10, 2023